Polymer Chemistry

PAPER

View Article Online
View Journal | View Issue

Cite this: *Polym. Chem.*, 2017, **8**, 5100

A mechanistic investigation of Pickering emulsion polymerization†

Andrea Lotierzo and Stefan A. F. Bon *

Received 22nd February 2017,
Accepted 25th March 2017

DOI: 10.1039/c7py00308k

rsc.li/polymers

Pickering emulsion polymerization offers a versatile way of synthetising hybrid core–shell latexes where a polymer core is surrounded by an armour of inorganic nanoparticles. A mechanistic understanding of the polymerization process is limited which restricts the use of the technique in the fabrication of more complex, multilayered colloids. In this paper clarity is provided through an in-depth investigation into the Pickering emulsion polymerization of methyl methacrylate (MMA) in the presence of nano-sized colloidal silica (Ludox TM-40). Mechanistic insights are discussed by studying both the adsorption of the stabiliser to the surface of the latex particles and polymerization kinetics. The adhesion of the Pickering nanoparticles was found not to be spontaneous, as confirmed by cryo-TEM analysis of MMA droplets in water and monomer-swollen PMMA latexes. This supports the theory that the inorganic particles are driven towards the interface as a result of a heterocoagulation event in the water phase with a growing oligoradical. The emulsion polymerizations were monitored by reaction calorimetry in order to establish accurate values for monomer conversion and the overall rate of polymerizations (R_p). R_p increased for higher initial silica concentrations and the polymerizations were found to follow pseudo-bulk kinetics.

Introduction

Waterborne nanocomposite polymer dispersions in which the particles are composed of a mixture of a polymeric and an inorganic phase (often a metal oxide) are an interesting class of materials. The use of water as continuous phase has environmental benefits, and the dual nature of these particles allows for performance enhancement of application products such as coatings and adhesives. For instance, hybrid particles can add magnetic response[1–3] and improve flame retardant and mechanical properties of dried films.[4,5] Furthermore, poly(lauryl acrylate) latex particles armoured with LAPONITE® clay discs have been shown to increase the tack adhesion of pressure-sensitive adhesives, when used as additive.[6] Surprisingly, the increase in mechanical properties was higher than when the inorganic and organic components were present as separate entities, suggesting a synergistic effect of the intricate core–shell armoured morphology. This widens the design window for intricately structured hybrid latex particles and their possible applications, including all those cases where inorganic materials are used in combination with polymers. Among them, the addition of (modified) silica nanoparticles in coatings resulted in the improvement of dirt pick-up,[7] and optical properties[8] and scratch resistance.[9]

The approaches adopted for the waterborne synthesis of nanocomposite polymer latexes generally differ in whether the polymerization and/or the synthesis of the inorganic component is conducted *in situ* or *ex situ*.[10,11] One morphology type of hybrid particles are armoured polymer colloids in which a polymeric core is surrounded with an inorganic layer. A synthetic strategy towards these particles is Pickering stabilization, a phenomenon whereby particles adhere to a soft deformable interface of, for example, an emulsion droplet.[12–14] The use of such particles as Pickering stabilizers in heterogeneous polymerization processes was first described by Rohm and Trommsdorff in 1934–35.[15] In their work, the authors used talc, barium sulphate, kaolin clay and aluminium oxide in the suspension polymerization of a variety of monomers. Since then Pickering hetero-phase polymerization has been developed further and now includes mini-emulsion,[16–18] dispersion[19,20] and emulsion polymerization processes,[21–27] using a variety of monomers and with a range of fillers, such as silica, LAPONITE® clay, magnetite, titanium dioxide, graphene oxide.[28] One driver for the development of heterogeneous Pickering polymerization processes is that they do not require molecular surfactants, offering a big advantage to the paint

Department of Chemistry, University of Warwick, Coventry, CV4 7AL, UK. E-mail: s.bon@warwick.ac.uk; http://www.bonlab.info

†Electronic supplementary information (ESI) available: Additional SEM and cryo-TEM pictures, graphs showing the variation of R_p with conversion (X), of the particles dispersity (PdI) with time and of number of nucleated particles with the silica content, derivation of eqn (8). See DOI: 10.1039/c7py00308k

industry as surfactant migration often deteriorates the performance of coatings.[29]

In particular, Pickering emulsion polymerization is an attractive synthetic route to fabricate hybrid armoured particles of sub-micron size. This process presents advantages over the Pickering mini-emulsion strategy which consists of the polymerization of Pickering-stabilized emulsion droplets, pre-formed during a high-shear emulsification step. The preparation of the mini-emulsion is not trivial to scale up, one reason being the abrasive nature of hard nanoparticle sols under high shear emulsification conditions. In Pickering emulsion polymerization, however, the hybrid latex particles are formed during the polymerization process. This makes the technique easily scalable and has therefore gained considerable interest.

A clear mechanistic understanding of the Pickering emulsion polymerization process is slowly emerging, but a number of key questions are still outstanding. Thorough knowledge of the mechanistic pathway and kinetic events would allow for the design of more complex particle morphologies, where different polymers and fillers can be combined to aid the fabrication of more advanced waterborne colloidal materials.

In this paper we will (1) address how the Pickering inorganic stabilizer ends up on the surface of the polymer particle, and (2) have an in-depth look at the overall polymerization kinetics of the Pickering emulsion polymerization of methyl methacrylate in presence of silica nanoparticles.

Experimental

Materials

Methyl methacrylate (MMA) and styrene (purities ≥98%) were purchased from Sigma Aldrich and filtered through basic aluminium oxide to remove the inhibitor. Methacrylic acid (≥98%), acrylamide (≥98%), hydroxypropyl methacrylate (mixture of isomers, 97%), di(ethylene glycol) ethyl ether acrylate (90% aq.), 2-hydroxyethyl methacrylate (97%), ammonium persulfate (APS) (98%), hexadecane (≥99%), colloidal nano silica Ludox TM-40 ($d \approx 25$ nm, aq. 40 wt%), were purchased from Sigma Aldrich and used as received. Hydrochloric acid (HCl, aq. 37 wt%) was supplied by Fisher Scientific.

Equipment

All the emulsion polymerizations were carried out in a calorimetry reactor consisting of a 1 L vacuum jacketed reactor (Radleys Ltd) equipped with a PFTE three blade impeller (Cowie Ltd) and three high precision Pt100 temperature probes (Omega Engineering inc. and Radleys Ltd). The three probes measure the temperature of the circulating fluid (silicon oil, kinematic viscosity at 20 °C = 10.8 $mm^2\ s^{-1}$, Julabo GmbH) in the inlet and outlet of the jacket of the reactor and inside the reactor. These probes are connected to a temperature logger that records and displays the temperatures every second. Extra insulating material (nitrile rubber, thickness 13 mm, RS Components Ltd) is present around the reactor main body and on the lid. The reactor was run in isoperibolic mode; the temperature of the jacket ($T_{avg,J}$) was kept constant and the reactor temperature (T_r) followed the reaction profile. The silicon oil flux was high and around 11 L min^{-1} in a way to mimimize the temperature difference between the inlet ($T_{J,in}$) and outlet ($T_{J,out}$) of the jacket.

A Branson 450 W digital sonifier was used to make oil-in-water mini-emulsions. pH measurements were taken on a pH benchtop meter A211 (Thermo Scientific Orion). Average particle sizes and distributions were measured by dynamic light scattering (DLS) using a Malvern Zetasizer Nano. Scanning electron microscopy (SEM) and cryogenic transmission electron microscopy (cryo-TEM) analyses were performed on a Zeiss Supra 55-VP FEGSEM and a Jeol 2200FS TEM, respectively.

Calorimetric data analyses

The energy balance equation for a batch calorimetry reactor is given by:

$$Q_{acc} = Q_{st} + Q_r - Q_J - Q_{loss} \quad (1)$$

where Q_{acc} is the heat rate accumulated in the reactor, Q_{st} represents the heating due to stirring (here assumed to be zero), Q_r is the heat rate of reaction, Q_J is the heat flow through the reactor wall due to the energy exchange between the reaction medium and the circulating fluid and Q_{loss} is the energy dissipated by the system. Note that all heats are expressed as power, in J s^{-1}.

Q_{acc} and Q_J can be calculated from the following expressions:

$$Q_{acc} = \frac{dT_r}{dt}\left(\sum c_{p,i} m_i\right) \quad (2)$$

$$Q_J = UA(T_r - T_{avg,J}) \quad (3)$$

where $c_{p,i}$ is the heat capacity at the temperature T of the i component and m is its mass, U is the global heat transfer coefficient, A is the surface area of the contact wall between the reaction mixture and the circulating fluid.

Knowing Q_r, the instantaneous monomer conversion (X) can then be estimated:

$$X = \frac{\int_0^{t_i} dQ_r}{\int_0^{t_f} dQ_r} X_{grav,f} \quad (4)$$

where $X_{grav,f}$ is the final conversion obtained by gravimetry. This term is added to correct for the actual final conversion of the reaction, otherwise the integrated ratio always equals 1.[30]

Just as in the commercial reactor calorimeter RC1 (Mettler Toledo), UA was calculated before and after every reaction and this two point calibration was used to account for its variation during the reaction.[30,31] Instead of using an electrical heater like in the RC1 reactor, UA was measured from temperature ramps before and after the polymerization.[32] As reported in the literature,[33] UA can be estimated by plotting $\ln((T_J - T_0)/(T_J - T_{r,i}))$ *vs.* time during a heating

ramp. *UA* can be then obtained from the slope of the resulting straight line:

$$\text{Slope} = \frac{UA}{\sum c_{p,i} m_i} \quad (5)$$

UA was found to vary from 3.70 ± 0.06 J K^{-1} s^{-1} before the polymerization to 2.61 ± 0.24 J K^{-1} s^{-1} after it. The feasibility of this method along with the accuracy of the calculated values were checked with an electrical heater using a procedure explained elsewhere.[34] A value of 4.5 ± 0.1 J K^{-1} s^{-1} was found using just deionized water. The approach adopted here allows us to calculate *UA* in reaction conditions and takes into account the volume contraction due to polymerization and solvent evaporation. Q_{loss} was determined by imposing Q_r to be 0 before the initiator injection (Fig. S1†). In this way, Q_{loss} was found to be 2.76 ± 0.25 J s^{-1}.

Typical Pickering emulsion polymerization protocol

86.0 g of silica nanoparticles (214.9 g of Ludox TM-40, aq. 40 wt%) was diluted in 557.7 g of water and the pH of the sol was adjusted to 3.5 using conc. HCl (aq.). The dispersion was poured into the reactor, the reactor was sealed and the void volume was purged with nitrogen gas for 10 minutes. The reaction mixture was further purged for 35 minutes under stirring at 225 rpm. The monomer (MMA, 85.8 g) was separately purged for 15 minutes and injected into the system. The reactor was heated up to 61–62 °C (circulator set to 63 °C) for 2 hours to reach steady state conditions (with respect to temperature). 3.0 ml of purged deionised water was heated to 75 °C and added to a purged sealed vial containing APS (0.117 g). The resulted solution was then immediately injected into the reactor to start the polymerization.

Samples (typically 1 g) were withdrawn throughout the polymerization to check monomer conversion *via* gravimetry.

Mini-emulsions preparation

36.0 g of Ludox TM-40 was diluted with 144.0 g of deionized water in a glass jar and the pH of the suspension was adjusted to 3.5–4.5 using concentrated HCl. (aq.) 16.5 g of MMA was added to the suspension along with 1.3 g of hexadecane to suppress Oswald ripening (8.0 wt% with respect to MMA).[35] The suspension was sonicated under vigorous stirring at 70% amplitude for 3 minutes with 30 s wait every 30 s. The jar was immersed in an ice bath during the sonication to prevent temperature rise.

Results and discussion

Pickering emulsion polymerization is too often erroneously associated to the polymerization of monomer droplets stabilized by inorganic particles. The latter should rather be called Pickering suspension polymerization, or if the armoured droplets are small, Pickering mini-emulsion polymerization. Instead, in Pickering emulsion polymerization the Pickering stabilizer is wrapped onto the surface of the latex particles during their formation and growth resulting in an armoured morphology (see Fig. 1). In order to unravel the mechanism of how such hybrid latex particles are formed, a series of experiments were designed using methyl methacrylate or styrene as monomer and silica nanoparticles (Ludox TM-40) as Pickering stabilizer. We divide our results and discussion into two sections. Firstly, the adsorption of the inorganic particles onto monomer droplets and the interface of the latex particles is discussed. In this section, the wettability of growing oligoradicals with the Pickering stabiliser in the water phase is discussed using styrene as a reference hydrophobic monomer. Secondly, data on the overall Pickering emulsion polymerization of methyl methacrylate in presence of the silica nanosol is presented.

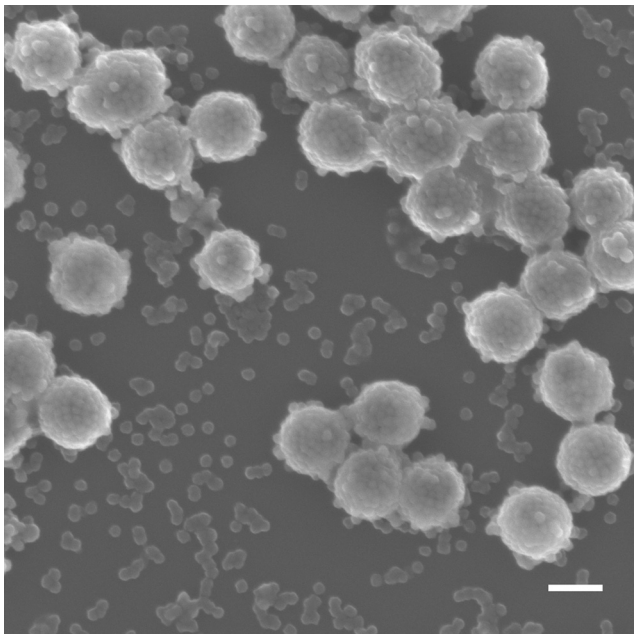

Fig. 1 SEM image of PMMA–SiO_2 nanocomposite armoured latex particles obtained *via* Pickering emulsion polymerization. Scale bar 200 nm.

On the adsorption of the Pickering stabilizer onto monomer droplets and latex particles

In a characteristic Pickering emulsion polymerization experiment, a water-based sol of colloidal silica adjusted to acidic pH is added to a 1 L reactor along with the monomer, in this study methyl methacrylate, and they are stirred together using an impeller or anchor blade at 200–300 rpm. Through continuous agitation, a coarse dispersion of micrometric size droplets in water is formed. In principle, silica nanoparticles could adsorb at the monomer–water interface forming a Pickering stabilized emulsion. In the literature, it has been suggested that this would be the case for the Pickering emulsion polymerization of styrene using nano-sized silica particles as Pickering stabilizer and in the presence of poly(ethylene glycol) mono methyl ether methacrylate as comonomer.[25] The same was claimed for the system of styrene in the presence of LAPONITE® clay,[36] and the copolymerization of MMA and

n-butyl acrylate in the presence of glycerol-functionalized silica and a cationic initiator.[21]

On the contrary, we believe this is not necessarily the case in our system. In exploratory experiments there seemed to be no difference in the stability of the coarse emulsion generated when stirring together water and methyl methacrylate in the absence or presence of silica. In both cases, the monomer droplets phase separated within minutes. It could be argued from this observation that the silica nanoparticles do not adsorb. This is not trivial for the following reason. When we consider a single emulsion droplet (of say 100 μm in diameter) and calculate its terminal velocity and assume in the crudest way that collision of this droplet with any stagnant interface, for example the upper air–water interface, occurs through full dissipation of kinetic energy, energy values (*ca.* $7700kT$) easily exceed the values needed to remove the nanosilica from the MMA–water interface.

To investigate whether or not silica nanoparticles spontaneously adhere to droplets of MMA, we prepared 3 mini-emulsions of 10 wt% MMA (containing 8 wt% hexadecane to retard Ostwald ripening) in water by applying a great input of energy to the system through ultrasound. The first two mini-emulsions were prepared in the presence (A) and absence (B) of silica nanoparticles. In the third (C) system, the nano-silica was added after sonication. Next, the mini-emulsions were stored for 21 days at room temperature, after which the image in Fig. 2 was taken. Note that these mini-emulsions were not polymerized.

After preparation of mini-emulsions (B) and (C), a number of large monomer droplets emerged rapidly at the top of the vials through coalescence and creaming. After ageing, these two emulsions showed a clear layer of monomer at the air/water interface (Fig. 2), indicating that substantial coalescence of the monomer droplets had occurred. The remaining opacity is logical as the distance travelled through buoyancy of small MMA droplets (<300 nm in diameter) is <5.8 mm. Emulsion (C) was more opaque than (B), probably due to the presence of the silica nanoparticles. On the contrary, the first mini-emulsion (A) contained no layer of monomer at the air/water interface. Instead, the mini-emulsion seemed to have partially sedimented. For this to happen, the monomer droplets need to have a density greater than water, as in the case for small MMA droplets armoured with a layer of silica nanoparticles. The presence of silica nanoparticles on the surface of the MMA droplets from mini-emulsion (A) was confirmed by cryo-TEM analysis (see Fig. 3). Strikingly, no settling of mini-emulsion (C) was observed, indicating that spontaneous adhesion of silica nanoparticles to droplets of MMA does not occur. This would suggest the presence of an energy barrier against spontaneous adsorption of silica nanoparticles onto to MMA droplets as a result to the electrostatic repulsion between a negative SiO_2 nanoparticle approaching the interface and the negatively charged surface of a monomer droplet.[37] In fact, it has been previously shown that the presence of the double layer provides an electrostatic barrier and can retard or prevent the adsorption of particles at soft interfaces.[38,39] The intensity of this barrier can be surprisingly higher than the hydrodynamic forces pushing the particle towards the droplet.[40,41] As a result of that, even in the presence of weak forces, external work must be often applied *via* high shear or sonication in order to observe adsorption of particles at a reasonable rate, which would confirm our results.[41,42] Furthermore, curvature effects may play a role. This is because the difference in pressure between the inside and the outside of the 200 nm droplet, the so called Laplace pressure, is 1000 times higher with respect to a 200 μm droplet and the mean Gaussian curvature is be 10^6 times higher.[43] This difference will result in the presence of a less flexible interface that may further hinder the adsorption process.

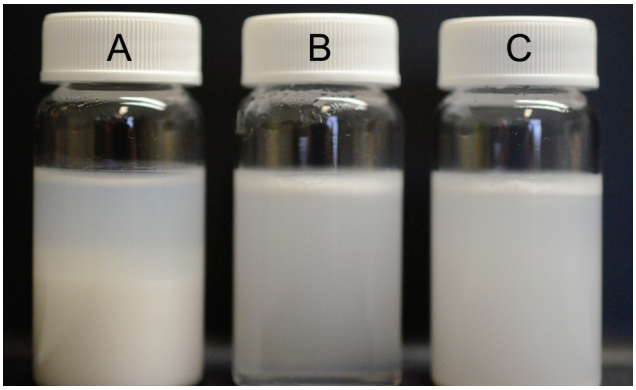

Fig. 2 Three mini-emulsions of MMA in water (8 wt% hexadecane with respect to MMA) prepared through emulsification by ultrasound. Emulsion (A) was emulsified in the presence of nanosized silica and the other two (B and C) in the absence of. In the case of emulsion (C), the stabilizer was added afterwards.

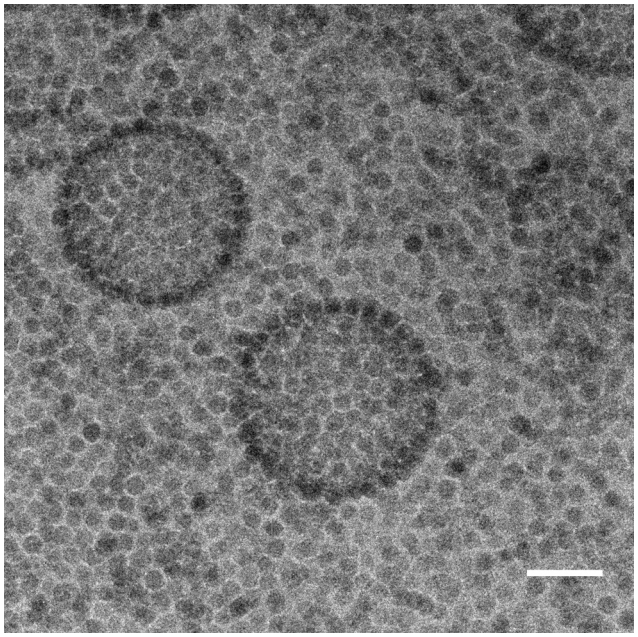

Fig. 3 (a) Cryo-TEM image of silica armoured MMA droplets in water obtained through sonication of a mixture of MMA and water in the presence of a silica nanosol (Ludox TM-40). Scale bar 100 nm.

If silica does not spontaneously adhere to monomer droplets, would the same hold for adsorption onto the surface of a swollen latex particle? Answering this question is of key importance in unravelling the mechanism of Pickering emulsion polymerization. In fact, during stage two of a conventional emulsion polymerization process (Harkins classical model) polymer latex particles swollen with monomer are the loci where the polymerization takes place.[44] In a typical Pickering emulsion polymerization experiment if the reaction conditions allow so (*i.e.* if enough stabilizer is present), the nucleated particles are surrounded by Pickering stabilizers from the first stages of the polymerization and they appear fully covered when they grow.[21,22] An explanation for this behaviour was that upon growth, newly generated 'naked' surface area lowers colloidal stability. The inorganic particles would then adsorb on the latex particle to aid stability, hence acting as Pickering stabilizers. If this explanation was true, the silica should in principle adsorb spontaneously onto the surface of a latex made by conventional emulsion polymerization which, if fully swollen with monomer, simulates particle growth in stage 2 of the emulsion polymerization process. We found that this is not the case. Cryo-TEM analysis of a soap-free dialyzed PMMA latex fully swollen with MMA in the presence of silica Ludox TM-40 at acidic pH (see Fig. S2;† see also Fig. S3a† for SEM) shows the absence of silica particles on the surface of the latex. This suggests that the above proposed mechanism for the silica adsorption during particle growth is at least partially incorrect, and that spontaneous adhesion of silica nanoparticles does not happen in the absence of additional attractive forces (*e.g.* Coulombic attraction). Interestingly, when in a similar experiment, swollen PMMA latex particles were mixed with silica Ludox TM-40 and exposed to sonication, latex particles covered in silica were observed, and no naked particles were found (Fig. S3b†). These two results reinforce the hypothesis of an energy barrier against adsorption. In case of swollen particles additional surface charge, due to for example initiator fragments,[45] enhances this barrier.

Our results clearly show that spontaneous adhesion of the silica nanoparticles does not occur. The outstanding question is, "how do the silica nanoparticles end up on the surface of the latex particles in a Pickering emulsion polymerization process?" We previously reported[22] that a possible mechanism for the adsorption of a Pickering stabilizer onto a latex particle could be the precipitation of a growing polymer chain in the water phase onto a silica nanoparticle followed by heterocoagulation with the growing latex particle. A similar mechanism involving the same heterocoagulation event was theorized by Sheibat-Othman *et al.*[25] and Thickett *et al.*[26]

If this mechanism for particle adhesion onto the latex particles is true, it can be expected that the change in wettability properties of the growing oligomeric radicals in the water phase have the ability to tune the efficiency of the adsorption process. To illustrate this concept we exchanged MMA for styrene, which is more hydrophobic, and should lead to naked particles upon emulsion polymerization in presence of silica sol. Small amounts (up to 3 wt%) of hydrophilic comonomers were used to tailor the chemical composition and thus wettability of growing oligomers in the water phase. The outcome on whether or not armored particles were obtained is presented in Table 1.

In the absence of any functional comonomer, indeed naked latex particles were observed (Fig. 4a). The only comonomer that improved SiO_2 adsorption onto the surface was di(ethylene glycol) ethyl ether acrylate (DEGEEA). Interestingly, it was also found that the increase of its concentration from 1.0 wt% to 3.0 wt% led to higher surface coverage (Fig. 4b and c). A good explanation is the strong attractive interaction between the pendant ethylene oxide units and the silica surface.[46]

Table 1 Comonomers used in the Pickering emulsion polymerization of styrene in presence of SiO_2. The polymerizations were carried out overnight at 65 °C, pH 5, at a styrene solid content of 10 wt% and SiO_2/M = 1.00 w/w

Comonomer	Wt%[a]	Coverage
Methacrylic acid (MAA)	1.0	None
	3.0	None
Di(ethylene glycol) ethyl ether acrylate (DEGEEA)	1.0	Partial
	3.0	Full
MAA/DEGEEA 1/1 w/w	1.0	None
Acrylamide	3.0	None
2-Hydroxyethyl methacrylate (HEMA)	3.0	None
Hydroxypropyl methacrylate (HPMA)	3.0	None

[a] Weight ratio with respect to styrene.

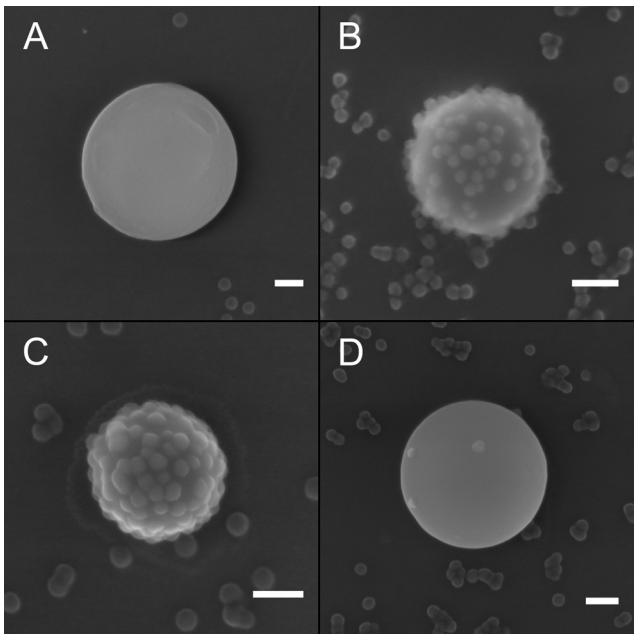

Fig. 4 SEM images of the latex particles resulting from the Pickering emulsion polymerization of styrene (a) in the absence of comonomer, in the presence of (b) 1.0 wt% (with respect to styrene) and (c) 3.0 wt% of di(ethylene glycol) ethyl ether acrylate, in the presence of (d) 1.0 wt% of MAA. Additional pictures can be found in the ESI (Fig. S4†). Scale bars 100 nm.

Whereas hydroxypropyl methacrylate (HPMA) is too hydrophobic, surprisingly the more hydrophilic 2-hydroxyethyl methacrylate (HEMA) was not effective. In the case of acrylamide, the reason why this comonomer led to poor results may originate from unfavourable reactivity ratios. Methacrylic acid (MAA) is hydrophilic and can promote interaction with silica through H-bonding.[23] However, under reaction conditions, pH *ca.* 5, the carboxylic acid groups are partially dissociated and the charge repulsion between the negatively charged carboxylic groups and the silica surface seemed to be the predominant effect. When a mixture of 0.5 wt% of DEGEEA and 0.5 wt% of MAA the effects cancelled out, and naked particles were obtained.

One point to address is whether or not a particle can desorb once it is on the surface of a monomer droplet or an armoured particle. We mixed an armoured PMMA–SiO_2 nanocomposite latex (prepared according to the recipe reported in the Experimental section) with a naked soap-free PMMA latex and stirred the suspension overnight. No redistribution of silica particles was found, confirming what elegantly shown by Balmer and coworkers.[47,48] In addition, we added sodium dodecyl sulfate to the PMMA–SiO_2 armoured latex and left the sample in an ultrasound bath at 37% frequency for 5 min. Again, all the latex particles were still covered in nanosilica. Moreover, extreme dilution of the sample in water did not show any desorption of the stabilizer, even after 6 months. This implies that dynamic partitioning is prohibited confirming that the silica nanoparticles are tightly bound to the surface.

In summary, we conclude that the Pickering emulsion polymerization process itself drives the adhesion of silica onto the latex particles, with waterborne oligomeric propagating radicals acting as mediators. The adsorption of silica onto the surface was shown not to occur spontaneously on the latex surface under the investigated conditions. This supports the theory of a heterocoagulation event between a growing oligoradical and a silica nanoparticle. Such an event would change the wetting properties of the Pickering stabilizer that would then be able to adhere to the latex surface.

This implies that at any reaction time there can never been more silica particles adhered to the surface than the total number of radicals generated. In order to illustrate this point, we consider a reaction initiated in 671.00 g of water by 0.12 g of APS at 61 °C ($k_d = 6.2 \times 10^{-6}$ s^{-1}).[49] After 10 min of reaction time, 2.2×10^{17} radicals would be produced when an initiator efficiency of 0.1 is used to account for the fraction of radicals actually undergoing entry. A typical experiment shows an average particle size of 100 nm in diameter and approximately 1.0×10^{16} armoured latex particles at this stage of the emulsion polymerization process. A calculation of the total number of silica nanoparticles adhered to the surface of the armoured latex particles yields a value of 2.1×10^{17} (packing parameter $P = 0.909$). The comparison of this value with the amount of radicals generated is striking and reinforces our mechanistic insight. Note that the radical efficiency of APS is usually higher and in the range 0.1–0.4,[50,51] still validating our statement.

On the overall rate of polymerization in Pickering emulsion polymerizations

In section 1, we come to an understanding on what the drivers are for the silica nanoparticles to adhere to the surface of the latex particles. What requires discussion is how the presence of the Pickering stabilizers influences the overall rate of polymerization in the emulsion polymerization process. In other words, how particle nucleation and growth are modified by the presence of the Pickering stabilizer.

A series of emulsion polymerizations of MMA in the presence of varying amounts of SiO_2 nanoparticles were run. MMA was chosen because with this monomer, armoured latex particles can be formed without the need of an auxiliary comonomer.[24] The polymerizations were performed at different silica-to-monomer ratios (SiO_2/M). The water-to-monomer ratio and initiator concentration were kept constant (see Table 2).

The SiO_2/M ratio was varied from 0.10 to 2.00 w/w and a polymerization without SiO_2 was also performed as a reference. The theoretical solid content in the absence of silica was 12.5 wt% based on full conversion of MMA. At this solid content and in the absence of any stabilizer, the system lost colloidal stability in the final stage of the emulsion polymerization (monomer conversion (X) > 0.8) and completely coagulated. SEM analysis of a sample taken at the end of the reaction showed that secondary nucleation occurred (see Fig. 5c). In other words, in the later stages of the polymerization process a second crop of particles emerged. This event triggered the observed coagulation.

In all the experiments in the presence of the nano-sized silica sol, armoured core–shell particles were obtained (illustrative examples are provided with Fig. 5a and b). No coagulation was observed in these Pickering emulsion polymerizations, with the exception of the two experiments carried out at the lowest silica loadings. In SiO_2/M = 0.10 w/w full coagulation arose at approximately 40% monomer conversion and clusters of 2 or more fused particles were observed (Fig. 5b). In the case of SiO_2/M = 0.50 w/w micro-coagulation was observed, characterized by small dispersed flocks of clustered particles (Fig. S5†). Fully stable latexes were obtained with SiO_2/M = 0.75 w/w or higher (Fig. 5a).

Table 2 Pickering emulsion polymerization of MMA using different amounts of SiO_2. The polymerization was carried out at 63 °C for 2–3 h. The monomer/water ratio was kept constant at 12.5 wt%. The $(NH_4)_2S_2O_8$ concentration in water was 0.76 mM

SiO_2/M (w/w)	m_{water}/g	m_{silica}[a]/g	d_Z/nm	PdI/—
2.00	428.8	429.8	460	0.105
1.50	493.2	322.3	382	0.071
1.00	557.7	214.9	349	0.076
0.75	589.9	161.2	356	0.088
0.50	622.2	107.6	1033	0.253
0.10	673.7	21.5	2281	0.882
0.00	686.6	0.0	845	0.269

[a] Mass of silica sol 40 wt% (Ludox TM-40).

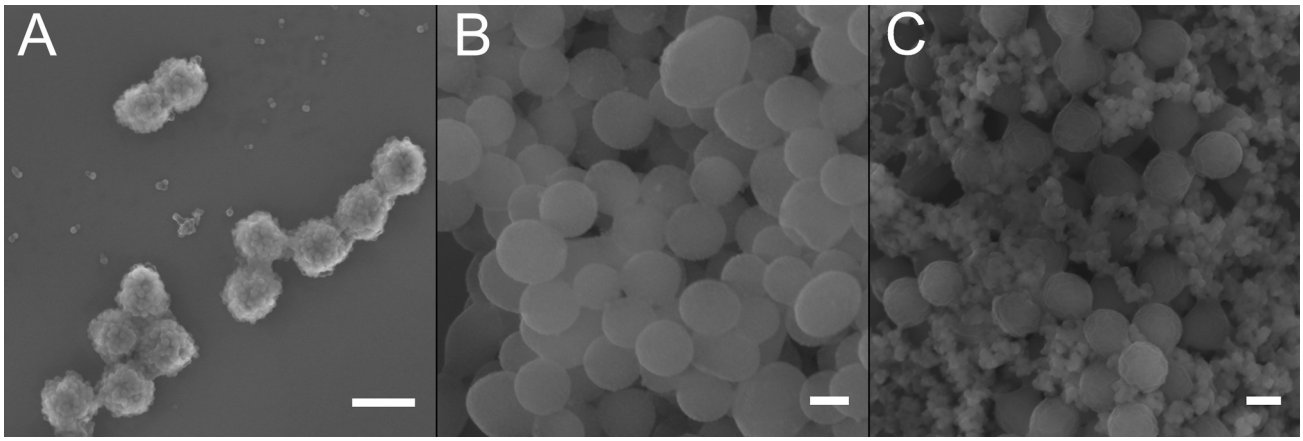

Fig. 5 SEM pictures of latex nanoparticles formed in the case of (a) SiO_2/M = 1.50 w/w, (b) SiO_2/M = 0.10 w/w, (c) SiO_2/M = 0.00 w/w. Scale bars 300 nm.

The performed emulsion polymerizations were followed online by reaction calorimetry. The instantaneous heat of reaction Q_r was measured using the heat balance equation described in the Experimental section (see Fig. 6a). All the curves present a region of steady polymerization followed by a sudden steep increase in Q_r attributed to the occurrence of the gel effect, or Trommsdorff–Norrish effect.[52] The gel effect is caused by a rise in the reaction rate caused by a drop in the rates of diffusion. The occurrence of this phenomenon in the free radical polymerization of MMA is known to take place at about 20–30% of monomer conversion,[53] as supported by our data. This auto-acceleration proceeds until high monomer conversion (that is $X > 0.8$) when the combination of the increase in viscosity of the system and the reduction in the monomer concentration and intraparticle diffusion eventually slows the overall polymerization process down. It can be noticed that with the given system and the used calibrations a full monitoring of the polymerization through the whole reaction time was tedious. The drastic drop in temperature after the occurrence of the gel effect is such that the calculated Q_r values after this point are negative even though the reaction has not reached full conversion yet (Fig. S1†). For the purpose of our discussion we will focus on stages on the polymerization up to 80% conversion, for which our calculated values for monomer conversion (using eqn (5)) are in excellent agreement with independent gravimetric data (see Fig. 6b).

An initial look at the reaction heat and monomer conversion data shows that addition of a small amount of silica to the system (SiO_2/M = 0.10 w/w) already led to a considerable shortening of the time required to reach the glassy state and high monomer conversion with respect to the reference system in absence of any stabilizer. Further additions of silica progressively played a smaller role in the reduction of the overall polymerization time until its influence became almost negligible. Similar results were reported by Teixeira *et al.*[23] and by

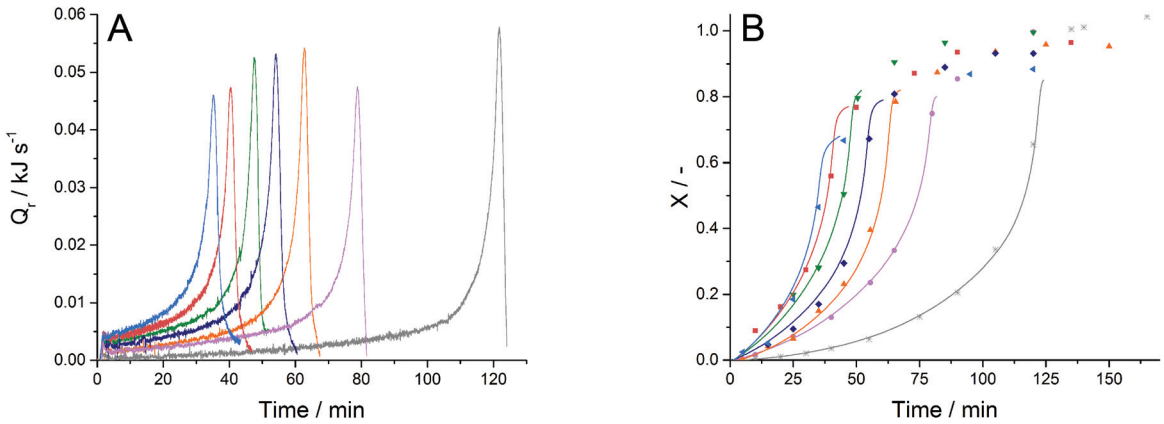

Fig. 6 (a) Variation of the heat of reaction (Q_r) for the Pickering emulsion polymerization of methyl methacrylate (MMA) in the presence of different initial nanosilica/MMA weight ratios (SiO_2/M); (b) estimated monomer conversion from calorimetry data (lines) compared to conversion measured from gravimetry samples withdrawn during the reaction (points). SiO_2/M = 0.00 (grey), 0.10 (pink), 0.50 (orange), 0.75 (dark blue), 1.00 (green), 1.50 (red), 2.00 (light blue) w/w.

Bourgeat-Lami *et al.*[27] using LAPONITE® clay in the polymerization of styrene/*n*-butyl acrylate and styrene, respectively.

When we take a closer look at Fig. 6a and b, higher rates of polymerization are observed at low to intermediate monomer conversion when larger amounts of silica are used. The overall rate of polymerization (R_p) for the Pickering emulsion polymerization of MMA in the presence of different SiO_2 amount is shown in Fig. 7. Roughly R_p increased with a factor of 3 moving from the polymerization in absence of stabilizer to the one with the highest amount. The rate is reported for conversion (X) values between 5% and 20%. The reason for this is that for $X > 20\%$ the influence of the Trommsdorff–Norrish effect greatly affects the reaction kinetics (Fig. S6†). For $X < 5\%$ the signal noise due to the initiator injection is high, especially for the fastest experiments. In addition, for very low conversions new particles are still nucleating, resulting in an additional increase in R_p.

R_p can be calculated from conversion data using eqn (6):

$$R_p = \frac{dX}{dt}\frac{mol_M}{V_{H_2O}} = \frac{k_p N_p C_{p,M} \bar{n}}{N_A} \quad (6)$$

where mol_M are the initial moles of monomer, V_{H_2O} is the volume of water, k_p is the rate coefficient of the monomer, N_p is the number of latex particles per litre of water, $C_{p,M}$ is the concentration of the monomer within the particles, $\bar{n}$ is the average number of radicals per particle and N_A is the Avogadro number.

The origin of the 3-fold increase in R_p for higher silica loadings can be explained by a number of factors. One could argue higher values of k_p as the faster polymerization lead to higher temperatures in the reactor. However, this effect was restricted within a 2 K temperature range, not explaining our observed increase. In addition, we make the reasonable assumption that $C_{p,M}$ is constant (6.6 M for PMMA latexes, according to Gilbert).[54] This means that the reason for the observed increase in R_p has to do with compartmentalization and thus the number of particles and their size. Hence, the nanoparticles play a prime role in the latex particles formation stage of Pickering emulsion polymerization.

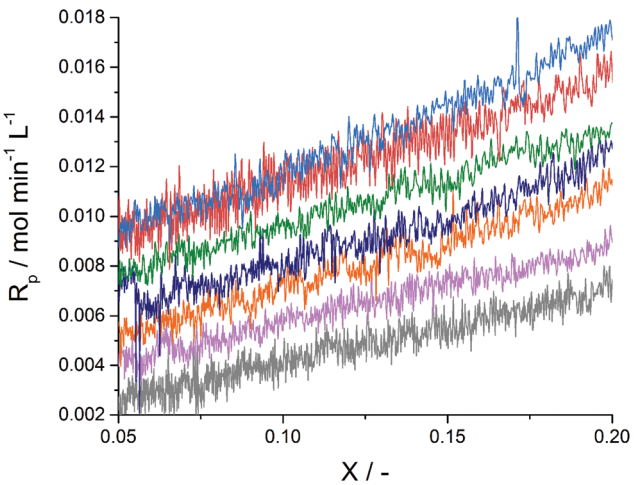

Fig. 7 Variation in the polymerization rate (R_p) until 20% conversion for the Pickering emulsion polymerization of MMA in the presence of nanosilica. SiO_2/M = 0.00 (grey), 0.10 (pink), 0.50 (orange), 0.75 (dark blue), 1.00 (green), 1.50 (red), 2.00 (light blue) w/w. A broader look at the reaction rates until about 80% conversion can be found in the ESI (Fig. S6†).

Particle nucleation in soap-free emulsion polymerization follows a homogeneous nucleation mechanism (the so-called HUFT theory).[55] According to this mechanism, primary particles form from growing radicals in water that phase separate from solution after having reached the critical chain length (j_{crit}) at which they are insoluble and precipitate as a primary particle.[55] These primary particles can subsequently assemble into larger coalesced clusters, hereby minimizing their free energy by decreasing the overall surface area. In a similar way, Pickering emulsion polymerization has been proposed to follow an analogous nucleation mechanism. In this case, different primary particles coagulate with one another, but now the Pickering stabilizer can participate. We previously suggested that a growing oligomeric radical could adhere to the Pickering stabilizer, under the conditions of favourable wetting of the nanoparticle with the polymer chain.[22] This concept is supported by our results on the adhesion of silica nanoparticles onto polystyrene latexes in the presence of various auxiliary hydrophilic monomers (see Fig. 4 and Table 1). Further propagation of the adhered polymer chains renders the Pickering stabilizer more hydrophobic, triggering its active participation in the latex particle formation process. A similar mechanism has been also suggested by Bourgeat-Lami *et al.*[25] for polystyrene/SiO_2 and poly(styrene-*co*-methyl methacrylate)/SiO_2 nanocomposites formed in the presence of poly(ethylene glycol) methyl ether methacrylate and Fielding *et al.*[21] for the copolymerization of methyl methacrylate and *n*-butyl acrylate using glycerol functionalized silica and 2,2′-azobis(2-methylpropionamidine) as initiator.

If this mechanistic path was correct, it would explain how these hybrid particles are always covered by silica during their growth; oligoradicals would be formed in the water phase throughout the whole length of the polymerization providing new silica particles that could adsorb at the bare polymer–water interface. Furthermore, this mechanism would better explain the difference in silica surface packing density between the polystyrene–SiO_2 hybrid latex shown in Fig. 4b and the PMMA–SiO_2 shown in Fig. 5a. The reason for this could be the quick consumption of the more hydrophilic comonomer from the water phase in the early stages of the reaction in the former case. This would initially lead to a given amount of silica nanoparticle adsorbing at the surface initially that then would remain constant during particle growth. In the case of PMMA, growing oligoradicals would be formed in the water phase, as long as monomer molecules are present in the water phase and these SiO_2–polymer "janus" structures would be captured by existing particle surrounded or not by silica nanoparticles.

We followed the particle size distribution throughout the Pickering emulsion polymerization process, the results of which are displayed in Fig. 8. From this it is evident that the addition of the Pickering stabilizer resulted in a marked

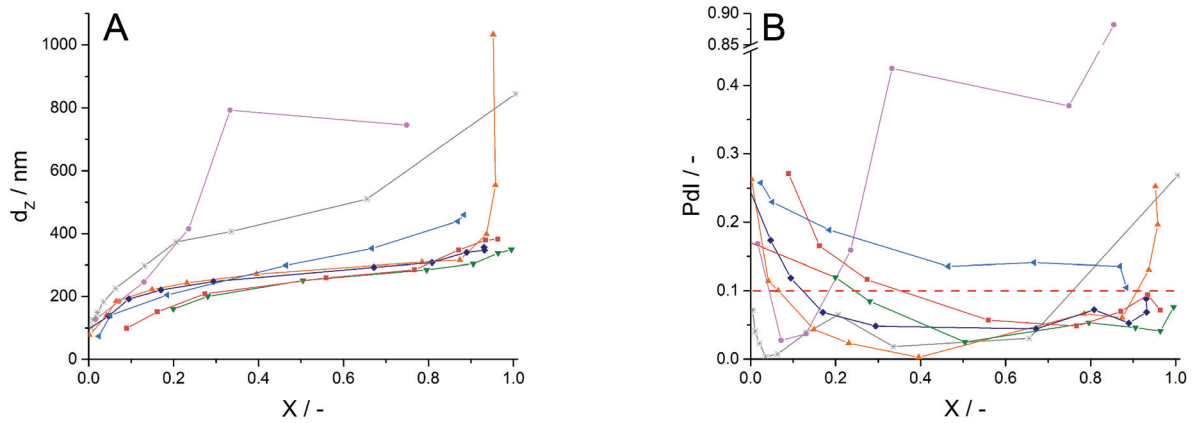

Fig. 8 Pickering emulsion polymerization of MMA in the presence of different silica/monomer ratios (SiO_2/M); (a) variation of the hydrodynamic diameter (d_Z) with X; (b) variation of the particle dispersity (PdI) with X. SiO_2/M = 0.00 (grey), 0.10 (pink), 0.50 (orange), 0.75 (dark blue), 1.00 (green), 1.50 (red), 2.00 (light blue) w/w.

reduction of the average particle size, and thus a greater number of latex particles. This supports the above mechanism of latex particle nucleation. For $SiO_2 \geq 0.75$ w/w, similar particles sizes were observed, phasing out the effect of the stabilizer on the final latex size. When we look at the particle size dispersity (PdI) (Fig. 8b) two things are worth mentioning. Firstly, the increase in dispersity sometimes observed at higher monomer conversion is directly associated with coagulation. For example, when 0.10 w/w Ludox silica nanoparticles with respect to monomer is used, the onset of coagulation already occurs at above $X = 0.15$. The second observation is the initial drop in dispersity as a function of monomer conversion, seemingly extending to greater values of X when more silica is used. One could infer a prolonged nucleation period when more silica is used, extending up to 40% conversion. When dispersity is plotted *vs.* time (Fig. S7†), however, the effects overlap with one another. A more plausible explanation is the interference of the scattering data obtained from the silica nanoparticles and the armoured latex particles. We therefore argue that nucleation is relatively fast. This is supported by the data in Fig. 7, where the slopes of R_p *vs.* X roughly are identical for values of $X > 0.05$, ruling out more prolonged nucleation events at greater silica to monomer ratios.

One final remark is that at the highest silica to monomer ratios, that is 2.00, a deviation from the "phase-out" trend becomes apparent. The viscosity increased noticeably during the reaction due to the high targeted solid content of 37.5 wt%. The reaction did not coagulate but the PdI was higher and around 0.10–0.15. The particles were also about 100 nm larger than the ones with lower SiO_2 loading (for SiO_2/M > 0.50 w/w). Therefore, it appears that there is a window for the amounts of Pickering stabilizer that can be used.

Knowing R_p, $\bar{n}$ can be calculated by rearranging eqn (6). In order to do this, the total number of nucleated particles per litre of water (N_p) is needed. We calculated values for N_p using DLS data with the following protocol. An approximate final diameter of the nanocomposite latex particles was obtained by plotting d_z^3 against X and extrapolating the final latex diameter to $X = 1$ (Fig. S7†). In fact, in the absence of secondary nucleation d_z should show a third order dependence with X because conversion scales with mass, which scales with volume, which scales with d_z^3. Essentially, in the absence of secondary nucleation d_z^3 *vs.* X plots should be linear. The extrapolation of the diameter for $X = 1$ gives an estimate of the final particles diameter in the absence of particle–particle interaction or aggregation at high conversion. From this, N_p was calculated with this simple expression, taking into account a correction for the silica shell:

$$N_p = \frac{6m_{M,0}}{\pi(d_Z - d_{SiO_2})^3 \rho_p} \quad (7)$$

where $m_{M,0}$ is the initial mass of monomer and ρ_p is the polymer density.

N_p calculated in this way confirmed what was previously observed; the addition of a small amount of SiO_2 brought to a drastic increase in N_p, which was then rapidly phased out for increasing stabiliser initial concentrations (Fig. S8†). These values also phase out upon further additions of stabiliser. The experiment conducted with the highest silica-to-monomer ratio (SiO_2/M = 2.00 w/w) showed a reduction in N_p, but we believe this was an artefact. The latex produced in this case had a higher than expected viscosity, indicating micro-coagulation, which explains the apparent drop in the value for N_p.

The obtained values for $\bar{n}$ for the Pickering emulsion polymerization of MMA in the presence of nanosilica are presented in Fig. 9. All reactions showed expected pseudo-bulk kinetics, with a linear increase in $\bar{n}$ for all the runs. This is in agreement with the behaviour observed in conventional emulsion polymerization of MMA.[54] Ballard and coworkers argued that for low values of $\bar{n}$ this trend could be quantified with a dimensionless acceleration parameter. Theoretically a value of 0.5 for this parameter is obtained in the case of emulsion polymerization with complete re-entry of desorbed free rad-

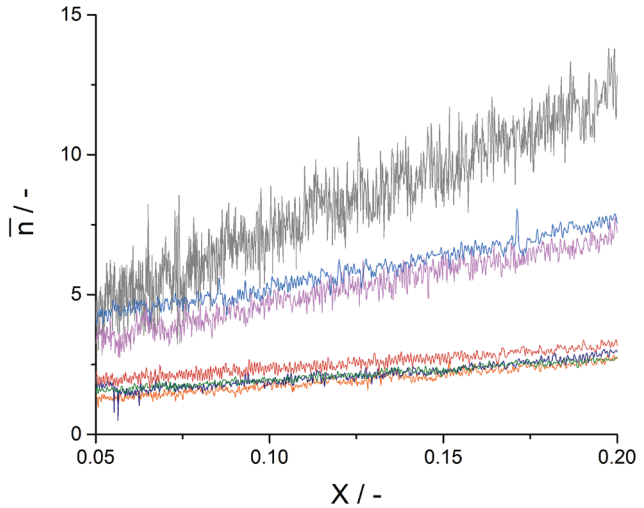

Fig. 9 Variation in the average number of radicals per particle ($\bar{n}$) between 5 and 20% conversion for the Pickering emulsion polymerization of MMA in the presence of nanosilica. SiO_2/M = 0.00 (grey), 0.10 (pink), 0.50 (orange), 0.75 (dark blue), 1.00 (green), 1.50 (red), 2.00 (light blue) w/w.

icals. We obtained calculated values between 0.3–0.6 for all runs with the exception of the silica-free standard emulsion polymerization, in agreement with values obtained from conventional emulsion polymerization reactions.[54] This is logical as the substantially larger particles lead to high values of $\bar{n}$ for which the theoretical value of 0.5 for the acceleration parameter is no longer valid.

We would like to point out that the calculated values for $\bar{n}$ are sensitive to the values of N_p used. In case of the runs that showed partial coagulation, that is SiO_2/M = 0.10 (pink) and 2.00 (light blue), N_p was underestimated, leading to too high values of $\bar{n}$.

In the last part of this paper we would like to make some more comments on particle nucleation, in line with our comment that at any reaction time there can never been more silica particles adhered to the surface of the latex particles than the total number of radicals generated. As we showed, the nucleation process is strongly influenced by the presence of silica nanoparticles dispersed in the water phase. At the end of Pickering emulsion polymerizations of methacrylates there is an excess of stabilizer left in the water phase.[24] One could argue then that the presence of substantial amounts of Pickering stabilizer would lead to prolonged nucleation periods. However, latexes with a relatively low dispersity in size are obtained.

Taking a step back, in conventional soap-free emulsion polymerization particle nucleation stops when growing oligoradicals are captured exclusively by existing latex particles through entry.[49] This happens when the total surface area of the latex particles is large enough to prevent further aqueous phase propagation, which leads to the formation of new primary particles. Coming back to Pickering emulsion polymerization, let's assume that the only fate for a growing oligoradical in the water phase would be either to "enter" a silica nanoparticle, sticking to it under the conditions of favourable wetting, or to enter a latex particle. The ratio between these two entry events would be proportional to the total surface areas of the silica and the latex particles. We would like to introduce this ratio f (eqn (8)) as a measure to understand particle formation. f was derived from our previous equation to predict the SiO_2 concentration in the water phase during Pickering emulsion polymerization (see ESI†).[24] It is worth mentioning that eqn (8) takes into account the decrease in silica concentration in the water phase due to the adsorption of the stabilizer onto the latex particles.

$$f = \frac{m_{SiO_2,0}\rho_p\left(d_{L,t} - d_{SiO_2}\right)^3}{m_{M,0}X_t\rho_{SiO_2}d_{SiO_2}{d_{L,t}}^2} - \frac{\pi\left(d_{L,t} - d_{SiO_2}\right)^2}{{d_{L,t}}^2 P\beta} \quad (8)$$

where $m_{SiO_2,0}$ is the initial mass of silica; ρ_{SiO_2} is the silica density; $d_{L,t}$ and d_{SiO_2} are the nanocomposite particle and the silica average diameters according to DLS; X_t is the monomer conversion at the time t; P is a packing parameter and β is a correction factor to account for the non-smooth nature of the raspberry-type particles and the use of the hydrodynamic diameters instead of the actual ones.

This parameter essentially describes the likelihood for a growing oligoradical bumping into a silica nanoparticle with respect to a nanocomposite particle. The variation of f with monomer conversion is shown in Fig. 10. We previously described that a possible nucleation mechanism for Pickering emulsion polymerization would be the heterocoagulation of growing oligoradicals in the water phase on silica nanoparticles, with a possible post rearrangement of these colloidal objects into primary nanocomposite particles. Keeping this in mind, at the beginning of the reaction entering a silica nanoparticle is the preferential option for a growing chain as no polymer particles are present yet. The value of f decreases quickly during particle formation due to nucleation of new particles surrounded by silica. According to Fig. 10, f would

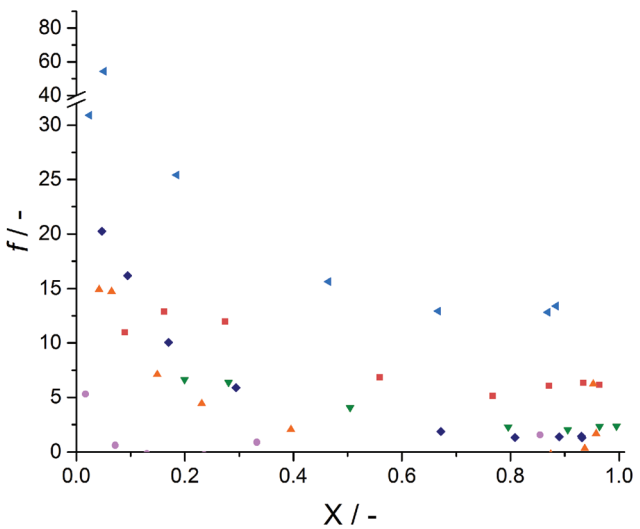

Fig. 10 Variation of the ratio f (silica/nanocomposite particles surface area) as a function of monomer conversion (X) for the Pickering emulsion polymerization of MMA and nanosilica.

normally reach a value between 0 and 5, implying that the formation of new particles would be slower and drastically suppressed but would never cease. However, our calculated values for f are crude estimates, as we assume a packed monolayer of silica on the armoured latexes, and rely on the accuracy of dynamic light scattering data. Moreover, we do not take into account any potential barrier towards the two entry events, which may favour one over the other. Therefore, the true f values can significantly vary from those reported in Fig. 10. Lower values would directly imply that nucleation would stop when it becomes less likely for a growing oligoradical to bump into a silica nanoparticle. In this way, the tendency of nucleating a second crop of particles is suppressed and the final PdI is low. This would be in agreement with our experiments. A closer look at the verified values for f obtained from actual Pickering emulsion polymerizations would offer greater understanding of particle nucleation. This, however, lies outside the scope of the current work.

Conclusions

In our studies we have come to the conclusion that the silica nanoparticles do not spontaneously adhere to latex particles. A key message is that the Pickering stabilizer needs wetting by means of adsorption of a growing radical from the water phase in order to trigger adhesion onto the growing latex particles. Furthermore, it was shown that the presence of Pickering stabilizers greatly influences the particle formation process.

This combined understanding can lead to the design of seeded Pickering emulsion polymerization experiments with the aim to fabricate more complex multi-layered latexes.

The measurements of the overall heat of reaction allowed us to come to an in depth understanding of the polymerization kinetics. It was shown that the Pickering emulsion polymerizations obeyed pseudo-bulk kinetics with an indication of full re-entry of desorbed radical species. The analogy to conventional emulsion polymerizations may indicate that the presence of the nanocomposite armour on the polymer latex does not severely restrict phase transfer events like entry/exit and monomer swelling.

Acknowledgements

Dulux Australia is acknowledged for funding (AL). The authors would also like to thank Dr Saskia Bakker for her help with Cryo-TEM analysis and acknowledge the University of Warwick Advanced BioImaging Research Technology Platform.

Notes and references

1 N. Yanase, H. Noguchi, H. Asakura and T. Suzuta, *J. Appl. Polym. Sci.*, 1993, **50**, 765–776.
2 Z. Xu, A. Xia, C. Wang, W. Yang and S. Fu, *Mater. Chem. Phys.*, 2007, **103**, 494–499.
3 K. Li, P. Y. Dugas, M. Lansalot and E. Bourgeat-Lami, *Macromolecules*, 2016, **49**, 7609–7624.
4 X. Zhou, H. Shao and H. Liu, *Colloid Polym. Sci.*, 2013, **291**, 1181–1190.
5 T. Kashiwagi, A. B. Morgan, J. M. Antonucci, M. R. Vanlandingham, R. H. Harris, W. H. Awad and J. R. Shields, *J. Appl. Polym. Sci.*, 2002, **89**, 2072–2078.
6 T. Wang, P. J. Colver, S. A. F. Bon and J. L. Keddie, *Soft Matter*, 2009, **5**, 3842.
7 M. V. Kharisovna and P. Wolfgang, EP2408864, 2012.
8 J. Moghal, S. Reid, L. Hagerty, M. Gardener and G. Wakefield, *Thin Solid Films*, 2013, **534**, 541–545.
9 F. Bauer, R. Flyunt, K. Czihal, M. R. Buchmeiser, H. Langguth and R. Mehnert, *Macromol. Mater. Eng.*, 2006, **291**, 493–498.
10 M. A. Hood, M. Mari and R. Muñoz-Espí, *Materials*, 2014, **7**, 4057–4087.
11 E. Bourgeat-Lami, *J. Nanosci. Nanotechnol.*, 2002, **2**, 1–24.
12 P. Finkle, H. D. Draper and J. H. Hildebrand, *J. Am. Chem. Soc.*, 1923, **45**, 2780–2788.
13 S. U. Pickering, *J. Chem. Soc. Trans.*, 1907, **91**, 2001–2021.
14 W. Ramsden, *Proc. R. Soc. London*, 1903, **72**, 156–164.
15 O. Rohm and E. Trommsdorff, US2171765A, 1939.
16 S. Fortuna, C. A. L. Colard, A. Troisi and S. A. F. Bon, *Langmuir*, 2009, **25**, 12399–12403.
17 S. A. F. Bon and P. J. Colver, *Langmuir*, 2007, **23**, 8316–8322.
18 S. Cauvin, P. J. Colver and S. A. F. Bon, *Macromolecules*, 2005, **38**, 7887–7889.
19 M. J. Percy, V. Michailidou and S. P. Armes, *Langmuir*, 2003, 2072–2079.
20 M. Gill, J. Mykytiuk, S. P. Armes, J. L. Edwards, T. Yeates, P. J. Moreland and C. Mollett, *J. Chem. Soc., Chem. Commun.*, 1992, 108–109.
21 L. A. Fielding, J. Tonnar and S. P. Armes, *Langmuir*, 2011, **27**, 11129–11144.
22 P. J. Colver, C. A. L. Colard and S. A. F. Bon, *J. Am. Chem. Soc.*, 2008, **130**, 16850–16851.
23 R. F. A. Teixeira, H. S. McKenzie, A. A. Boyd and S. A. F. Bon, *Macromolecules*, 2011, **44**, 7415–7422.
24 C. A. L. Colard, R. F. A. Teixeira and S. A. F. Bon, *Langmuir*, 2010, **26**, 7915–7921.
25 N. Sheibat-Othman and E. Bourgeat-Lami, *Langmuir*, 2009, **25**, 10121–10133.
26 S. C. Thickett and P. B. Zetterlund, *ACS Macro Lett.*, 2013, **2**, 630–634.
27 B. Brunier, N. Sheibat-Othman, Y. Chevalier and E. Bourgeat-Lami, *Langmuir*, 2016, **32**, 112–124.
28 A. Schrade, K. Landfester and U. Ziener, *Chem. Soc. Rev.*, 2013, **42**, 6823–6839.
29 D. Scalarone, M. Lazzari, V. Castelvetro and O. Chiantore, *Chem. Mater.*, 2007, **19**, 6107–6113.
30 L. V. De La Rosa, E. D. Sudol, M. S. El-Aasser and A. Klein, *J. Polym. Sci., Part A: Polym. Chem.*, 1996, **34**, 461–473.
31 S. BenAmor, D. Colombié and T. McKenna, *Ind. Eng. Chem. Res.*, 2002, **41**, 4233–4241.

32 E. Bourgeat-Lami, N. Sheibat-Othman and A. M. Dos Santos, *in Polymer Nanocomposites by Emulsion and Suspension Polymerization*, Royal Society of Chemistry, Cambridge, 2011, pp. 269–311.
33 F. X. McConville, *The Pilot Plant Real Book*, FXM Engineering and Design, 1st edn, 2002.
34 I. Saenz de Buruaga, A. Echevarha, P. D. Armitage, J. de la Cal, J. R. Leiza and J. M. Asua, *AIChE J.*, 1997, **43**, 1069–1081.
35 J. M. Asua, *Prog. Polym. Sci.*, 2002, **27**, 1283–1346.
36 N. Sheibat-Othman, A. M. Cenacchi-Pereira, A. M. Dos Santos and E. Bourgeat-Lami, *J. Polym. Sci., Part A: Polym. Chem.*, 2011, **49**, 4771–4784.
37 H. Wang, V. Singh and S. H. Behrens, *J. Phys. Chem. Lett.*, 2012, **3**, 2986–2990.
38 S. Kutuzov, J. He, R. Tangirala, T. Emrick, T. P. Russell and A. Böker, *Phys. Chem. Chem. Phys.*, 2007, **9**, 6351.
39 A. M. Rahmani, A. Wang, V. N. Manoharan and C. E. Colosqui, *Soft Matter*, 2016, **12**, 6365–6372.
40 S. Tcholakova, N. D. Denkov and A. Lips, *Phys. Chem. Chem. Phys.*, 2008, **10**, 1608.
41 A. Stocco, E. Rio, B. Binks and D. Langevin, *Soft Matter*, 2011, **4**, 1260–1267.
42 K. Du, E. Glogowski, T. Emrick, T. P. Russell and A. D. Dinsmore, *Langmuir*, 2010, **26**, 12518–12522.
43 P. C. Hiemenz and R. Rajagopalan, *Principles of Colloid and Surface Chemistry*, Taylor and Francis Group, 1997.
44 M. S. El-Aasser and P. A. Lovell, *Emulsion polymerization and emulsion polymers*, J. Wiley, 1997.
45 K. H. Van Streun, W. J. Belt, P. Piet and A. L. German, *Eur. Polym. J.*, 1991, **27**, 931–938.
46 N. Derkaoui, S. Said, Y. Grohens, R. Olier and M. Privat, *Langmuir*, 2007, **23**, 6631–6637.
47 J. A. Balmer, O. O. Mykhaylyk, J. P. A. Fairclough, A. J. Ryan, S. P. Armes, M. W. Murray, K. A. Murray and N. S. J. Williams, *J. Am. Chem. Soc.*, 2010, **132**, 2166–2168.
48 J. A. Balmer, E. C. Le Cunff and S. P. Armes, *Langmuir*, 2010, **26**, 13662–13671.
49 R. G. Gilbert, *Emulsion polymerization, a mechanistic approach*, Academic Press Inc., San Diego, 1995.
50 G. Moad and D. H. Solomon, *The chemistry of free radical polymerization*, Elsevier Science Inc., Oxford, UK, 2nd edn, 1995.
51 B. M. E. Van der Hoff, *J. Polym. Sci.*, 1960, **44**, 241–259.
52 E. Trommsdorff, H. Kohle and P. Langally, *Makromol. Chem.*, 1948, **1**, 169.
53 S. T. Balke and A. E. Hamielec, *J. Appl. Polym. Sci.*, 1973, **17**, 905–949.
54 M. J. Ballard, D. H. Napper and G. Robert, *J. Polym. Sci., Polym. Chem. Ed.*, 2006, **22**, 3225–3253.
55 R. M. Fitch, *Polymer Colloids: A Comprehensive introduction*, 1997.